favorably with experimental data than those of Ref. 9 but less favorably than those of Ref. 6. However, the results reported in this work as well as those reported in Refs. 6 and 9 correspond to Euler flow solutions, and as stated in Ref. 9, the modeling of the flow physics by the Euler equations is incomplete. In any case, given that our CFD mesh is coarser than both meshes employed in Refs. 6 and 9, that our ISS algorithm has the same computational complexity as the partitioned procedures used in these references, and that our time step is more than an order of magnitude larger than both time steps employed in Refs. 6 and 9, the results shown in Fig. 2 not only validate our aeroelastic computational methodology but also highlight its superior computational efficiency. Furthermore, they demonstrate that, for aeroelastic problems, a well-designed staggered algorithm can afford a time step that is comparable to that of a fully implicit monolithic scheme.

IV. Conclusions

It has often been stated that loosely coupled partitioned procedures for the solution of aeroelastic problems in the time domain are inferior to strongly coupled fully implicit monolithic schemes. We disagree with this viewpoint. Partitioned procedures and staggered algorithms offer the possibility to combine different solution methods that are tailored to the different mathematical models and geometric complexity underlying the fluid and structure problems, can take into account software availability in each individual discipline, simplify mixed explicit/implicit treatment, facilitate subcycling, preserve software modularity, and are the most if not the only feasible computational methods when the structural system is more complex than a simple airfoil or a homogeneous flat plate. We have presented a new enhanced staggered algorithm whose computational complexity is comparable to that of basic ones and yet allows the simplest partitioned procedure to operate with coupling time steps that are comparable to those afforded by fully implicit monolithic schemes. We have validated this algorithm with the flutter analysis of the AGARD wing 445.6 and have highlighted its superior accuracy and computational efficiency by proving it capable of operating accurately with a coupling time step that is 12.5–29 times larger than previously reported in the literature.

Acknowledgments

The authors acknowledge partial support by the National Science Foundation under Grants ASC-9217394 and ASC-9503301, partial support by RNR Numerical Aerodynamic Simulations at NASA Ames Research Center under Grant NAG 2-827, and partial support by the U.S. Air Force Office of Scientific Research under Grant F49620-97-1-0059.

References

[1]Farhat, C., Lesoinne, M., and Maman, N., "Mixed Explicit/Implicit Time Integration of Coupled Aeroelastic Problems: Three-Field Formulation, Geometric Conservation and Distributed Solution," *International Journal for Numerical Methods in Fluids*, Vol. 21, 1995, pp. 807–835.

[2]Morton, S. A., Melville, R. B., and Visbal, M. R., "Accuracy and Coupling Issues of Aeroelastic Navier–Stokes Solutions of Deforming Meshes," AIAA Paper 97-1085, April 1997.

[3]Piperno, S., Farhat, C., and Larrouturou, B., "Partitioned Procedures for the Transient Solution of Coupled Aeroelastic Problems," *Computer Methods in Applied Mechanics and Engineering*, Vol. 124, 1995, pp. 79–112.

[4]Strganac, T. W., and Mook, D. T., "Numerical Model of Unsteady Subsonic Aeroelastic Behavior," *AIAA Journal*, Vol. 28, 1990, pp. 903–909.

[5]Mouro, J., "Numerical Simulation of Nonlinear Fluid Structure Interactions Problems and Application to Hydraulic Shock-Absorbers," Third World Conf. Applied Computational Fluid Dynamics, Basel World User Days CFD, May 1996.

[6]Gupta, K. K., "Development of a Finite Element Aeroelastic Analysis Capability," *Journal of Aircraft*, Vol. 33, 1996, pp. 995–1002.

[7]Lesoinne, M., and Farhat, C., "Geometric Conservation Laws for Flow Problems with Moving Boundaries and Deformable Meshes, and Their Impact on Aeroelastic Computations," *Computer Methods in Applied Mechanics and Engineering*, Vol. 134, 1996, pp. 71–90.

[8]Yates, E. C., "AGARD Standard Aeroelastic Configuration for Dynamic Response, Candidate Configuration I.—Wing 445.6," NASA TM-100492, 1987.

[9]Lee-Rausch, E. M., and Batina, J. T., "Wing-Flutter Boundary Prediction Using Unsteady Euler Aerodynamic Method," AIAA Paper 93-1422, 1993.

[10]George, P. L., "Improvement on Delaunay Based 3D Automatic Mesh Generator," *Finite Elements in Analysis and Design*, Vol. 25, 1997, pp. 297–317.

R. K. Kapania
Associate Editor

Perturbation Method for Condensation of Eigenproblems

Ki-Ook Kim*
Inha University, Inchon 402-751, Republic of Korea

Introduction

DYNAMIC analysis of a large structural system involves structural matrices of large dimension and, hence, requires much computation. Powerful computers with effective numerical procedures such as parallel processing may be employed to obtain the exact solution. For general users, who have limited computing facilities and want to obtain the lowest eigenmodes, various reduction methods[1–3] have been used to transform the original eigensystem into a reduced subspace.

The reduced stiffness and mass matrices represent the conservation of the strain and kinetic energies of the structure. However, the energy distribution over the degrees of freedom is not exact, and the equation of motion in the reduced subspace does not satisfy the equilibrium of the original system.

Most research work has focused on making compromises between solution accuracy and computational efficiency. For a broad discussion of reduction methods for dynamic analysis, the reader is referred to the review of Ref. 4. General criteria have been suggested for the global approximation, which is the crux of reduction.

In system condensation, the secondary degrees of freedom are condensed out, and the reduced eigenproblem is expressed in terms of the primary ones. The major emphasis is put on how many and which degrees of freedom should be included in the primary set. The exact transformation between the primary and secondary sets should be different from mode to mode, which makes the computer implementation very difficult. Hence, the conventional transformation is assumed to be constant and becomes the main source of error.

The present study will closely examine the system transformation that has a great effect, in particular, higher modes. The perturbation equation, which is based on a correction of the transformation matrix, tends to push the condensation solution further to the exact one. Hence, the perturbation method is recommended as a supplementary step or postprocessor of condensation.

The method discussed here is similar, in principle, to the work of Flax[5] in which an accurate recovery of the secondary degrees of freedom was of great concern. The present Note seeks to establish a simple and systematic derivation of the perturbation equation. The perturbation method is revised to investigate the convergence characteristics of the condensation procedure and to propose a computational scheme for the improvement of the eigensolution.

Sometimes, numerical performance of condensation can be enhanced through the combined use of other reduction methods.[6,7] An advantage of integrated eigensolvers is that the influence of set selection in condensation can be attenuated through the subsequent solution procedures.

Condensation for Eigenproblems

In the finite element analysis, the equation of motion for undamped free vibration is written as a general eigenproblem:

$$[k]\{\phi\} = \lambda[m]\{\phi\} \tag{1}$$

Received Aug. 26, 1997; revision received May 15, 1998; accepted for publication May 20, 1998.

*Professor, Department of Aerospace Engineering. Senior Member AIAA.

where $[k]$ and $[m]$ are the stiffness and mass matrices. An eigenpair is denoted as λ and $\{\phi\}$. Equation (1) can be expressed in partitioned form as

$$\begin{bmatrix} k_{pp} & k_{ps} \\ k_{sp} & k_{ss} \end{bmatrix} \begin{Bmatrix} \phi_p \\ \phi_s \end{Bmatrix} = \lambda \begin{bmatrix} m_{pp} & m_{ps} \\ m_{sp} & m_{ss} \end{bmatrix} \begin{Bmatrix} \phi_p \\ \phi_s \end{Bmatrix} \tag{2}$$

The primary degrees of freedom $\{\phi_p\}$ are included in the analysis, whereas the secondary set $\{\phi_s\}$ is condensed out. The primary set should be able to describe the lowest eigenmodes accurately.

Two equations in Eq. (2) can be written explicitly as

$$\begin{aligned} ([k_{pp}] - \lambda[m_{pp}])\{\phi_p\} &= -([k_{ps}] - \lambda[m_{ps}])\{\phi_s\} \\ ([k_{ss}] - \lambda[m_{ss}])\{\phi_s\} &= -([k_{sp}] - \lambda[m_{sp}])\{\phi_p\} \end{aligned} \tag{3}$$

If the coefficient matrices are singular, there exist eigenvectors such that

$$([k_{pp}] - \lambda[m_{pp}])\{\psi_p\} = \{0\} \quad \text{or} \quad ([k_{ss}] - \lambda[m_{ss}])\{\psi_s\} = \{0\} \tag{4}$$

Then an arbitrary magnitude of $\{\psi_p\}$ (or $\{\psi_s\}$) may be added to $\{\phi_p\}$ (or $\{\phi_s\}$). In other words, one set can vibrate independently of the other. It is assumed that such local modes do not occur.

In Guyan's static condensation, the mass associated with the secondary set is assumed to be small. Hence, the stiffness matrix is used to get the transformation

$$\{\phi_s\} \cong -[k_{ss}]^{-1}[k_{sp}]\{\phi_p\} \equiv [T_0]\{\phi_p\} \tag{5}$$

Through the system transformation, an eigenproblem in the reduced subspace is obtained as

$$[K_r]\{\phi_p\} = \lambda_r[M_r]\{\phi_p\} \tag{6}$$

where

$$\begin{aligned} [K_r] &= [k_{pp}] - [k_{ps}][k_{ss}]^{-1}[k_{sp}] \\ [M_r] &= [m_{pp}] - [m_{ps}][k_{ss}]^{-1}[k_{sp}] - [k_{ps}][k_{ss}]^{-1}[m_{sp}] \\ &\quad + [k_{ps}][k_{ss}]^{-1}[m_{ss}][k_{ss}]^{-1}[k_{sp}] \end{aligned} \tag{7}$$

Because the transformation is not exact, λ_r may differ from λ.

Perturbation Equations for Condensation

In the static condensation, the exact transformation can be divided into two parts,

$$[T] = [T_0] + [\Delta T] \tag{8}$$

where

$$\begin{aligned} [T_0] &= -[k_{ss}]^{-1}[k_{sp}], \qquad [T_1] = [m_{sp}] + [m_{ss}][T_0] \\ [\Delta T] &= \lambda([k_{ss}] - \lambda[m_{ss}])^{-1}[T_1] \end{aligned} \tag{9}$$

where $[T_0]$ is the conventional transformation matrix. The corrective term $[\Delta T]$ contains the eigenvalue, and hence, the transformation should differ from mode to mode.

The corresponding perturbations of the reduced stiffness and mass matrices are written as

$$\begin{aligned} [\Delta K_r] &= [k_{ps}][\Delta T] + [\Delta T]^T[k_{sp}] + [T_0]^T[k_{ss}][\Delta T] \\ &\quad + [\Delta T]^T[k_{ss}][T_0] + [\Delta T]^T[k_{ss}][\Delta T] \\ &= \lambda^2[T_1]^T([k_{ss}] - \lambda[m_{ss}])^{-1}[k_{ss}]([k_{ss}] - \lambda[m_{ss}])^{-1}[T_1] \end{aligned} \tag{10}$$

$$\begin{aligned} [\Delta M_r] &= [m_{ps}][\Delta T] + [\Delta T]^T[m_{sp}] + [T_0]^T[m_{ss}][\Delta T] \\ &\quad + [\Delta T]^T[m_{ss}][T_0] + [\Delta T]^T[m_{ss}][\Delta T] \\ &= 2\lambda[T_1]^T([k_{ss}] - \lambda[m_{ss}])^{-1}[T_1] + \lambda^2[T_1]^T([k_{ss}] \\ &\quad - \lambda[m_{ss}])^{-1}[m_{ss}]([k_{ss}] - \lambda[m_{ss}])^{-1}[T_1] \end{aligned} \tag{11}$$

Hence, one obtains

$$[\Delta K_r] - \lambda[\Delta M_r] = -\lambda^2[T_1]^T([k_{ss}] - \lambda[m_{ss}])^{-1}[T_1] \tag{12}$$

A difficulty arises because the matrix inversion contains the eigenvalue. Therefore, the right-hand side is expanded using an infinite series,

$$[\Delta K_r] - \lambda[\Delta M_r] = -\lambda^2[T_2] - \lambda^3[T_3] - \lambda^4[T_4] - \cdots \tag{13}$$

where

$$\begin{aligned} [T_2] &= [T_1]^T[k_{ss}]^{-1}[T_1] \\ [T_3] &= [T_1]^T[k_{ss}]^{-1}[m_{ss}][k_{ss}]^{-1}[T_1] \\ [T_4] &= [T_1]^T[k_{ss}]^{-1}[m_{ss}][k_{ss}]^{-1}[m_{ss}][k_{ss}]^{-1}[T_1] \\ &\vdots \qquad\qquad\qquad\qquad \vdots \end{aligned} \tag{14}$$

The stiffness and mass matrices are usually symmetric and positive definite, and so are the matrices $[T_2], [T_3], [T_4], \ldots$.

The equilibrium equation for the perturbed subsystem is

$$[K_r']\{\phi_p'\} = \lambda_r'[M_r']\{\phi_p'\} \tag{15}$$

where

$$\begin{aligned} [K_r'] &= [K_r] + [\Delta K_r], \qquad [M_r'] = [M_r] + [\Delta M_r] \\ \{\phi_p'\} &= \{\phi_p\} + \{\Delta\phi_p\}, \qquad \lambda_r' = \lambda_r + \Delta\lambda_r \end{aligned} \tag{16}$$

The perturbation equation is exact for a specific mode of the eigenvalue $\lambda(=\lambda_r')$ used in Eqs. (9–12).

To show the nonlinear characteristics of the perturbed system, the perturbation equation is rearranged:

$$\begin{aligned} ([K_r] - \lambda_r[M_r])\{\Delta\phi_p\} &= -([\Delta K_r] - \lambda_r[\Delta M_r])\{\phi_p'\} \\ &\quad + \Delta\lambda_r([M_r] + [\Delta M_r])\{\phi_p'\} \end{aligned} \tag{17}$$

Neglecting the nonlinear terms, the first-order equation is obtained as

$$\begin{aligned} ([K_r] - \lambda_r[M_r])\{\Delta\phi_p\} &\cong -([\Delta K_r] - \lambda_r[\Delta M_r])\{\phi_p\} \\ &\quad + \Delta\lambda_r[M_r]\{\phi_p\} \end{aligned} \tag{18}$$

Using mass normalization for simplicity, one gets the eigenvalue change:

$$\Delta\lambda_r \cong \{\phi_p\}^T([\Delta K_r] - \lambda_r[\Delta M_r])\{\phi_p\} \tag{19}$$

Assuming $\lambda \cong \lambda_r$ in Eq. (13), the rate of eigenvalue change is obtained as

$$\Delta\lambda_r/\lambda_r \cong -\lambda_r C_1 - \lambda_r^2 C_2 - \lambda_r^3 C_3 - \cdots \tag{20}$$

where

$$\begin{aligned} C_1 &= \{\phi_p\}^T[T_2]\{\phi_p\} \\ C_2 &= \{\phi_p\}^T[T_3]\{\phi_p\} \\ C_3 &= \{\phi_p\}^T[T_4]\{\phi_p\} \\ &\vdots \qquad\qquad \vdots \end{aligned} \tag{21}$$

Equation (12) or (20) is similar to Eq. (11) of Ref. 5. Because the matrices $[T_2]$, $[T_3]$, $[T_4]$, ..., are positive definite, the values of C_i are positive, and the series should approach the exact eigenvalue from above.

However, numerical investigations reveal that several lowest terms in the series already overshoot the exact eigenvalue, and the approximation continues to decrease. It appears that the truncation of higher-order terms in the perturbation equation is the biggest cause, in addition to the assumption $\lambda \cong \lambda_r$.

Now it is assumed that

$$\lambda \cong \lambda_r' = \lambda_r + \Delta\lambda_r \tag{22}$$

Then, dropping the higher-order terms associated with $\{\Delta\phi_p\}$ gives the eigenvalue change as

$$\Delta\lambda_r \cong \{\phi_p\}^T([\Delta K_r] - \lambda_r'[\Delta M_r])\{\phi_p\} \tag{23}$$

For small $\Delta\lambda_r$, first-order terms are included to get

$$\frac{\Delta\lambda_r}{\lambda_r} \cong \frac{-\lambda_r C_1 - \lambda_r^2 C_2 - \lambda_r^3 C_3 - \cdots}{1 + 2\lambda_r C_1 + 3\lambda_r^2 C_2 + 4\lambda_r^3 C_3 + \cdots} \tag{24}$$

which gives a little improvement over Eq. (20). It is interesting that $\lambda_r C_1$ and $\lambda_r^2 C_2$ provide an excellent approximation in typical numerical problems.

The mode shape change $\{\Delta\phi_p\}$ is determined from Eq. (18). Because the coefficient matrix on the left-hand side of the equation is singular, a simple modification[8,9] is used to solve the equation.

The eigenvector expansion theorem shows

$$\{\Delta\phi_p\} = C_p\{\phi_p\} + \{W\} \tag{25}$$

where $\{W\}$ is the contribution of all of the mode shapes except $\{\phi_p\}$,

$$([K_r] - \lambda_r[M_r])\{W\} = -([\Delta K_r] - \lambda_r[\Delta M_r])\{\phi_p\} + \Delta\lambda_r[M_r]\{\phi_p\} \tag{26}$$

The self-contribution factor C_p is obtained using the mass normalization:

$$\begin{aligned} C_p &= -\tfrac{1}{2}\{\phi_p\}^T[\Delta M_r]\{\phi_p\} \\ &= -\tfrac{1}{2}\left(2\lambda C_1 + 3\lambda^2 C_2 + 4\lambda^3 C_3 + \cdots\right) \end{aligned} \tag{27}$$

Some of the nonlinear terms may be included to get a better estimation:

$$\begin{aligned} C_p &= -\frac{\{\phi_p\}^T[\Delta M_r]\{\phi_p\}}{2\left(1 + \{\phi_p\}^T[\Delta M_r]\{\phi_p\}\right)} \\ &= -\frac{\left(2\lambda C_1 + 3\lambda^2 C_2 + 4\lambda^3 C_3 + \cdots\right)}{2\left(1 + 2\lambda C_1 + 3\lambda^2 C_2 + 4\lambda^3 C_3 + \cdots\right)} \end{aligned} \tag{28}$$

The numerical procedure of the perturbation method can be summarized as follows:

1) The reduced eigenproblem in Eq. (6) is solved to get the eigenvalues.

2) $[T_i]$ in Eq. (14) and C_i in Eq. (21) are determined.

3) The eigenvalue change is calculated using Eq. (24).

4) The mode shape change is obtained in Eqs. (25), (26), and (28).

Convergence of Infinite Series

In practice, convergence of the matrices $\lambda^i[T_i]$ dictates the numerical performance of the perturbation equations. Although it takes computational effort to predict the variation of the matrices, the convergence characteristics can be roughly conjectured from the recurrent structure of the matrices:

$$\begin{aligned} &\left\|\lambda^3[T_3]\right\| \le \lambda/\lambda_s \left\|\lambda^2[T_2]\right\| \\ &\left\|\lambda^4[T_4]\right\| \le \lambda/\lambda_s \left\|\lambda^3[T_3]\right\| \le (\lambda/\lambda_s)^2 \left\|\lambda^2[T_2]\right\| \\ &\quad\vdots \qquad\qquad\qquad\qquad \vdots \end{aligned} \tag{29}$$

where $\|\ \|$ indicates a matrix norm and λ_s is the smallest eigenvalue in the subspace of the secondary degrees of freedom,

$$[k_{ss}]\{\psi_s\} = \lambda_s[m_{ss}]\{\psi_s\} \tag{30}$$

Fast convergence is obtained in lower modes, and the perturbation equation gives excellent results. In higher modes for which the ratio (λ/λ_s) is close to unity, however, it is difficult to overcome the limitation of slow convergence.

Numerical Examples

Cantilever Beam

Flexural vibration of a uniform beam (Fig. 1) is used to illustrate the method. Six nodes and five elements are used for the finite element modeling. The nodal displacement has 10 degrees of freedom for the planar motion of the beam. The primary set arbitrarily takes three translational degrees of freedom of nodes 2, 4, and 6.

Table 1 shows the numerical results for the first three eigenvalues. The static condensation gives good approximations, and substantial improvement is obtained through the perturbation procedure.

Helicopter Tail Boom

As an example of large systems, the tail-boom structure of the Cobra helicopter[10] is used. The finite element model consists of 28 nodes, 48 beam elements, and 8 concentrated masses. Figure 2 shows the geometrical layout of the tail boom.

The structure has 144 unconstrained degrees of freedom. The primary set contains the lateral translations of the eight nodes carrying the concentrated masses and has 16 degrees of freedom.

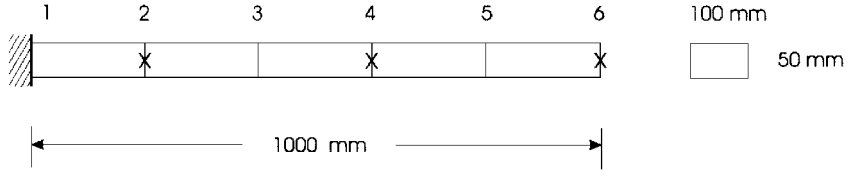

Fig. 1 Cantilever beam in flexural vibration: $E = 2.0684\ 10^5$ N/mm^2 and $\rho = 7.8334\ 10^{-9}$ N s^2/mm^4.

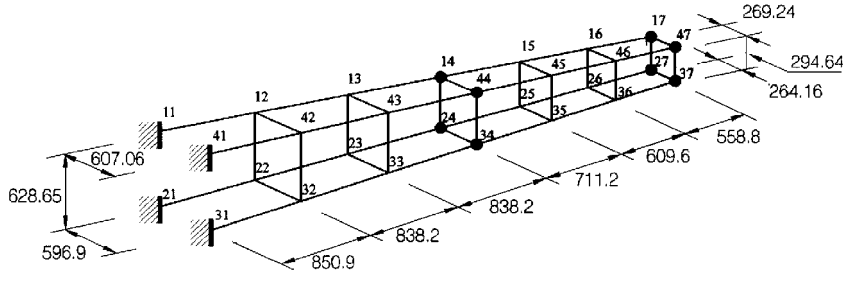

Fig. 2 Helicopter tail boom.

Table 1 Eigenvalues of cantilever beam

Mode	Exact	Condensation	Perturbation
1	6.80096×10^4	6.80933×10^4	6.80096×10^4
2	2.67360×10^6	2.75677×10^6	2.67364×10^6
3	2.10913×10^7	2.50865×10^7	2.11491×10^7

Table 2 Eigenvalues of tail boom

Mode	Exact	Condensation	Perturbation
1	1.72244×10^3	1.72259×10^3	1.72243×10^3
2	1.79624×10^3	1.79637×10^3	1.79620×10^3
3	8.76679×10^3	8.77111×10^3	8.76695×10^3
4	1.48218×10^4	1.48477×10^4	1.48219×10^4
5	1.51423×10^4	1.51703×10^4	1.51424×10^4
6	6.28409×10^4	6.29845×10^4	6.28423×10^4

Table 2 shows the first six eigenvalues. The static condensation gives excellent eigenvalues for up to six modes. The perturbation equation leads the approximation to the exact solution.

Conclusions

A perturbation method using a correction in transformation is presented to improve the condensation solution. The method proved to be effective and is recommended as a postprocessor of the condensation.

Theoretically, the perturbation solution should approach the exact eigenvalue from above. In practice, however, truncation error in the linear equation causes the approximation to overshoot the exact solution. Inclusion of several of the lowest terms can provide excellent estimations for both the eigenvalue and mode shape changes.

One of the most difficult problems is the rate of convergence in the series expansion. The sequential terms in the infinite series may indicate the convergence characteristics in an eigenvalue approximation.

Some of the nonlinear terms may be included to get more accurate solutions. Rather than iterations with nonlinear perturbation equations, integrated reduction methods such as the hybrid dynamic condensation are preferable.

Acknowledgment

This work was supported by Research Fund 1996 of Inha University.

References

[1]Guyan, R. J., "Reduction of Stiffness and Mass Matrices," *AIAA Journal*, Vol. 3, No. 2, 1965, p. 380.

[2]Leung, Y. T., "An Accurate Method of Dynamic Condensation in Structural Analysis," *International Journal for Numerical Methods in Engineering*, Vol. 12, No. 11, 1978, pp. 1705–1715.

[3]Suarez, L. E., and Singh, M. P., "Dynamic Condensation Method for Structural Eigenvalue Analysis," *AIAA Journal*, Vol. 30, No. 4, 1992, pp. 1046–1054.

[4]Noor, A. K., "Recent Advances and Applications of Reduction Methods," *Applied Mechanics Review*, Vol. 47, No. 5, 1994, pp. 125–146.

[5]Flax, A. H., "Comment on 'Reduction of Structural Frequency Equations,'" *AIAA Journal*, Vol. 13, No. 5, 1975, pp. 701, 702.

[6]"MSC/NASTRAN Handbook for Dynamic Analysis," MacNeal–Schwendler Corp., Los Angeles, CA, 1983.

[7]Kim, K. O., "Improved Hybrid Dynamic Condensation for Eigenproblems," AIAA Paper 96-1401, April 1996.

[8]Nelson, R. B., "Simplified Calculation of Eigenvector Derivatives," *AIAA Journal*, Vol. 14, No. 9, 1976, pp. 1201–1205.

[9]Kim, K. O., "Modal Design Sensitivities for Multiple Eigenvalues," *Computers and Structures*, Vol. 29, No. 5, 1988, pp. 755–762.

[10]Woo, T. W., "Space Frame Optimization Subject to Frequency Constraints," *AIAA Journal*, Vol. 25, No. 10, 1987, pp. 1396–1404.

R. K. Kapania
Associate Editor

Structural Approximate Reanalysis for Topological Modifications of Finite Element Systems

Suhuan Chen,* Cheng Huang,† and Zhongsheng Liu*
Jilin University of Technology,
Chang Chun 130022, People's Republic of China

Introduction

In a general layout optimization problem, possible modifications can be classified as follows[1]:

1) With deletion of members and joints, both the design variable vector and the number of degrees of freedom (DOFs) are reduced. If only members are to be deleted, the value of associated design variables becomes zero and can be eliminated from the set of variables.

2) With addition of members and joints, both the design variable vector and the number of DOFs are increased. When members are added without addition of joints, the vector of design variables is expanded, but the number of DOFs is unchanged.

3) With modification in the geometry, there is no change in the number of variables or in the number of DOFs. In this case, only the numerical values of the variable are modified.

Previous studies have addressed the described cases of layout modifications.[1–6] For the case of addition of members and joints (case 2), Kirsch and Liu[1] presented an effective method to establish a modified initial design. Even though it is suitable for changes in members of a truss structure, it is difficult to apply this method to other models of finite element systems.

In this Note, a new simple and convenient procedure is developed by introducing and reanalyzing the modified initial stiffness matrix (MISM), and a method for forming the expanded basis vectors is introduced. Using this approach, the MISM is formed directly by using the submatrices of an augmented stiffness matrix. Therefore, it is suitable for changes in a general finite element system. Once the MISM is introduced, an expanded basis vector is formed from the MISM; the combined approximations (CA) are used to give an approximate result of the modified structure. The CA method, used in previous studies for structural optimization,[1,5,6] is suitable for problems with unchanged numbers of design variables and DOFs. Because of the large changes involved in topological modification, third-order approximations (CA3) are used in this study. The calculations are based on results of a single exact analysis. Each subsequent reanalysis involves the solution of only a small system of equations. Thus, the computational effort is significantly reduced. In addition, evaluation of derivatives is not required.

Problem Formulation

Static analysis of the initial structure involves solving of a set of simultaneous equations

$$\boldsymbol{K}_0 \boldsymbol{u}_0 = \boldsymbol{R} \tag{1}$$

where $\boldsymbol{K}_0$ is the initial stiffness matrix and $\boldsymbol{u}_0$ is the initial displacement vector; the elements of the load vector $\boldsymbol{R}$ are assumed to be independent of the design variables. However, the approach presented here can also be used to deal with changes in the load vector. The initial stiffness matrix $\boldsymbol{K}_0$ is symmetric and banded, and its decomposition form is available:

$$\boldsymbol{K}_0 = \boldsymbol{L}_0 \boldsymbol{D}_0 \boldsymbol{L}_0^T \tag{2}$$

Received Dec. 15, 1997; revision received April 13, 1998; accepted for publication May 19, 1998.

*Professor, Department of Mechanics.
†Ph.D. Student, Department of Mechanics.